

**\*\*TITLE\*\***

*ASP Conference Series, Vol. \*\*VOLUME\*\*, \*\*YEAR OF PUBLICATION\*\**

**\*\*NAMES OF EDITORS\*\***

## Infrared Imaging Polarimetry of Massive Star-forming Regions

Bringfried Stecklum

*TLS Tautenburg, Sternwarte 5, D-07778 Tautenburg, Germany*

Thomas Henning, Markus Feldt

*MPIA, Königstuhl 17, D-69117 Heidelberg, Germany*

Hans-Ulrich Käuffl

*ESO, K.-Schwarzschild-Str. 2, D-85748 Garching, Germany*

Sebastian Wolf

*CALTECH, Mail Code 220-6, Pasadena, CA 91125, U.S.A.*

**Abstract.** Imaging polarimetry is a useful tool to reveal the 3D structure of dust distributions and to localize embedded young stellar objects (YSOs). We present maps of the linear polarization at  $2.2\ \mu\text{m}$  for three ultra-compact HII regions (UCHIIs, G192.16–3.82, G331.28–0.19, G339.88–1.26) and the methanol maser source G305.21+0.21. From the polarization maps, we draw conclusions on the morphology of these objects and the presence of luminous illuminating sources.

### 1. Introduction

Compared to the specific intensity, the polarization state of light provides additional information on the radiation field. Thus polarization measurements of light emerging from star-forming regions allow to retrieve important characteristics which can hardly be obtained otherwise. At near-infrared (NIR) wavelengths, scattering of light by dust grains is the primary polarization process. Single scattering may lead to high polarization degrees  $p$ , with  $p(\lambda)$  indicative for the grain size (Fischer et al. 1994). Since the vibration direction of the electric vector is perpendicular to the scattering plane defined by the incident and scattered rays, polarization measurements allow to localize the illuminating source, a technique which has been widely used for YSOs (e.g. Tamura et al. 1990; Burkert et al. 1998; Yao et al. 2000). Massive star-forming regions, particularly UCHIIs, harbor embedded star clusters (e.g. Feldt et al. 1998). Although the brightest object, i.e. the most massive star, might be hidden by dust, its scattered radiation can reach the observer if the extinction is non-isotropic since light emerging from directions of small optical depth will be scattered by grains into the line-of-sight. The position of the primary illuminator can be

estimated using the least-squares method of Perkins, King, & Scarrott (1981) or the centroid technique of Weintraub & Kastner (1993) which was applied for our targets. The positional uncertainty arises from measurement errors as well as from the contribution of scattered light from fainter stars, leading to both a decrease of the net polarization and a change of the position angle  $\Theta$  of the polarization vector compared to the case of a single source. Further depolarization can also be caused by multiple-scattering. By means of the NIR imaging polarimetry, we wanted to localize luminous embedded sources, study their relation with tracers of young, massive stars like methanol masers (e.g. Walsh et al. 1997), and look if discrete features represent stars or just scattering peaks.

## 2. Observations and data reduction

The observations were performed with SOFI at the ESO–NTT. The Wollaston prism produces two orthogonally polarized beams, separated by  $47''$  which match well the spatial extent of our targets. A slit mask avoids the overlapping of the two beams. Images at the pixel scale of  $0''.14$  were taken at five dithering positions using either the narrow-band filter  $2.195\ \mu\text{m}$  or the broad-band filter Ks. Observations at two instrument orientations yielded frames at polarization angles of 0, 45, 90 and  $135^\circ$ . The observing conditions were fine, with a seeing of  $\sim 0''.6$  and good transmission. The measurement of G339.88–1.26 was carried out in June 1998 while the other targets were observed in March 1999. The data processing included sky subtraction, flat-fielding using dome flats, and bad-pixel-correction. The target area was extracted for each polarization angle and the resulting four images were registered using stars in common. From the Stokes U and Q images the quantities  $p$  and  $\Theta$  were calculated according to the standard formulae (e.g. Fischer, Stecklum, & Leinert 1998), taking de-biasing into account (Wardle & Kronberg 1974). The polarization images were rebinned to a pixel size of  $0''.8$  to improve the signal-to-noise ratio (SNR). The astrometry was established on the full-field total intensity I frames based on either DSS or 2MASS and then transformed to the stack of smaller polarization frames. The astrometric error amounts to  $\sim 0''.2$ . For the estimation of the location of the illuminator only polarization vectors with  $p > 20\%$  (predominantly single scattering) in areas with  $I > 2\sigma$  were used. The error of this location is marked by the ellipse in the figures below.

## 3. Results

### 3.1. G192.16–3.82

This UCHII (IRAS 05553+1631) is caused by an early B star which is surrounded by an accretion disk (Shepherd et al. 2001). It drives a molecular outflow (Shepherd et al. 1998) oriented east-west. The polarization map (Fig. 1 left) shows a bipolar structure caused by scattering in the outflow cavities. The brightest NIR source is a scattering peak in the eastern cavity (blue-shifted outflow lobe) which is inclined toward the observer. Weaker scattered light is also detected from the western lobe. The centro-symmetry of the polarization pattern is distorted north of the brightest NIR source, presumably due to multiple

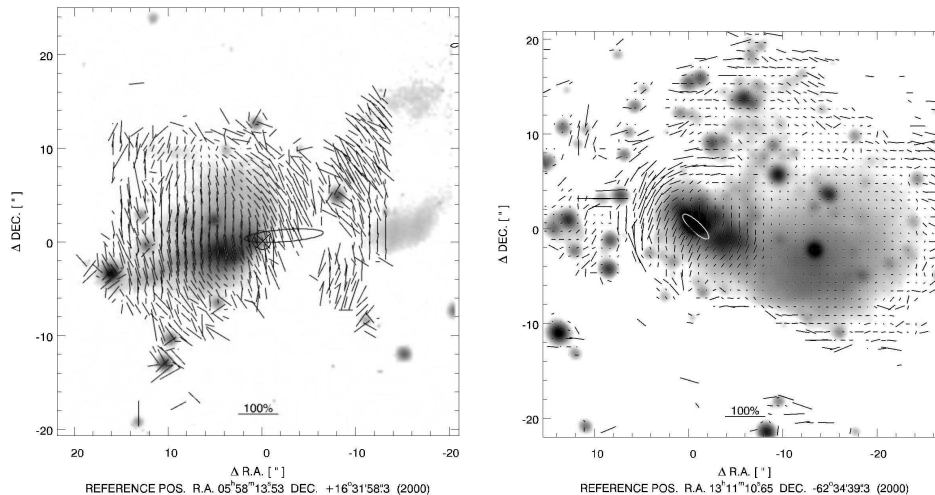


Figure 1. Left:  $2.195\ \mu\text{m}$  image of G192.16–3.82 with superimposed polarization map. The horizontal bar marks 100% polarization. The reference position (cross) corresponds to the peak of the 7 mm emission (Shepherd et al. 2001). The black contour delineates the 25% peak level of the 3.5 cm radio continuum (Kurtz 1995). Right: same for G305.21+0.21. The reference position corresponds to that of methanol masers of G305.202+0.207 (Norris et al. 1993).

scattering. The error ellipse includes both the UCHII and the peak of the 7 mm emission, confirming that the embedded object gives rise to these phenomena and the scattered light. A weak  $2.2\ \mu\text{m}$  source is detected at the reference position which might be the central star, barely seen along the rim of the eastern outflow cavity. The resolution of our images is not sufficient to prove whether or not it is a binary as suggested by Shepherd et al. (2001).

### 3.2. G305.21+0.21

This object (IRAS 13079–6218) harbors two centers of 6.7 GHz methanol maser emission. While the eastern one is not detected at IR wavelengths, the western one (G305.202+0.207, Fig.1 right) has a strong IR counterpart (Walsh et al. 2001). Strong polarization is present in the vicinity of the masers, indicating illumination from a compact source. At the presumed distance of 6.2 kpc (Phillips et al. 1998), the projected separation between the illuminator and the masers amounts to  $\sim 3000$  AU. The upper limit for its radio continuum emission corresponds to a spectral type later than B0.5 (Phillips et al. 1998). The MIR-to-radio flux ratio of the source exceeds that of normal star clusters, suggesting the presence of a “quenched” HII region (Walsh et al. 2001). The kinematics of the masers were interpreted in terms of a circumstellar disk (Phillips et al. 1998). The weak extended emission to the southwest coincides with a small HII region (Phillips et al. 1998) and is not strongly polarized. This might be due to diffuse illumination or a lack of dust grains. However dust cannot be completely absent since MIR radiation from this area has been observed (Walsh et al. 2001).

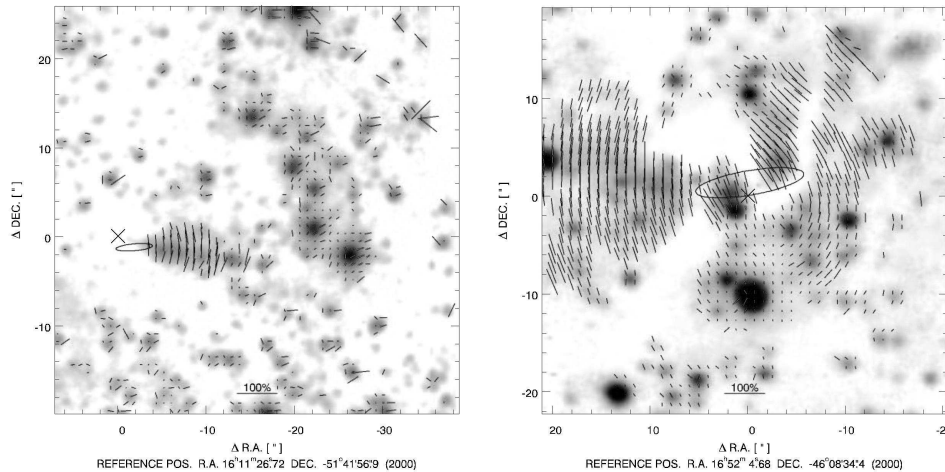


Figure 2. Left:  $2.195\ \mu\text{m}$  image of G331.28–0.19 with superimposed polarization map. Right: Ks image and polarization map of G339.88–1.26. For both objects the reference position corresponds to that of methanol masers (Norris et al. 1993).

### 3.3. G331.28–0.19

This methanol maser source (Fig. 2 left) has a  $10\ \mu\text{m}$  counterpart (Walsh et al. 2001). The associated 8.6 GHz radio continuum emission (Phillips et al. 1998) peaks  $3''$  south and points to the presence of a B0.5 star. At  $2.2\ \mu\text{m}$  a conical reflection nebula with a well-defined polarization pattern is obvious. The location of the illuminator coincides with that of the MIR source but is offset from the maser spots. The nebula is associated with  $\text{H}_2(1-0)\text{S}(1)$  emission, shifted in velocity with respect to the maser (Lee et al. 1999). A possible origin is a molecular outflow although fluorescent excitation cannot be ruled out. These features suggest that the object might be one of the youngest massive YSOs.

### 3.4. G339.88–1.26

This UCHII harbors a chain of 6.7 GHz methanol masers. The geometry and velocity gradient of the masers match the circumstellar disk model (e.g. Norris et al. 1998). Our  $10\ \mu\text{m}$  imaging seemed to support this view since it showed an elliptical object well aligned with the masers (Stecklum et al. 1998). De Buizer et al. (2000) arrived at a similar conclusion. Thus, the source was among the prime disk candidates. The polarization pattern (Fig. 2 right), however, is inconsistent with the presumed disk orientation. In those regions which would be shadowed by the hypothetical disk, highly polarized, nebulous emission is present. Our polarization data indicate that the star close to the maser location is not the main source as claimed by De Buizer et al. (2002) but a foreground object. The primary illuminator is situated behind a dust filament and thus hidden at NIR wavelengths. It seems likely that it corresponds to the object 1B of De Buizer et al. (2002).

#### 4. Conclusions

Our NIR imaging polarimetry of four massive star-forming regions yielded maps containing partial or almost complete centro-symmetric pattern of the polarization vectors. This implies the presence of a compact radiation source, either a single massive star or a dense cluster. These illuminators were detected at  $2.2\ \mu\text{m}$  for two targets but no NIR counterparts were found for the other two regions. In these cases, the young, massive stars are heavily obscured by dust which may reside in a broken-up cocoon or foreground filament. The luminous illuminating sources are very close to methanol masers proving that these masers are good tracers of early stages of massive star formation.

#### References

- Burkert, A., Stecklum, B., Henning, Th., & Fischer, O. 1998 *A&A* 353, 153  
De Buizer, J.M., Piña, R.K., & Telesco, C.M. 2000, *ApJS*, 130, 437  
De Buizer, J.M., Walsh, A.J., Piña, R.K., Phillips, C.J., & Telesco, C.M. 2002, *ApJ*, 564, 372  
Feldt, M., Stecklum, B., Henning, Th., Hayward, T.L., Lehmann, Th., & Klein, R. 1998 *A&A*, 339, 759  
Fischer, O., Henning, Th., & Yorke, H.W. 1994 *A&A*, 284, 187  
Fischer, O., Stecklum, B., & Leinert, Ch. 1998, *A&A*, 334, 969  
Kurtz, S. 1995, *RMxAC*, 3, 39  
Lee, J.K., Walsh, A.J., & Burton, M.G. 1999, in: *H<sub>2</sub> in Space*, ed. F. Combes & G. Pineau des Forêts (Cambridge Univ. Press), 65  
Norris, R.P., Whiteoak, J.B., Caswell, J.L., Wieringa, M.H., & Gough, R.G. 1993, *ApJ*, 412, 222  
Norris, R.P., & et al. 1998, *ApJ*, 508, 275  
Perkins, H.G., King, D.J., & Scarrott, S.M. 1981, *MNRAS*, 196, 7P  
Phillips, C.J., Norris, R.P., Ellingsen, S.P., & McCulloch, P M. 1998, *MNRAS*, 300, 1131  
Shepherd, D.S., Watson, A., Sargent, A., & Churchwell, E. 1998, *ApJ*, 507, 861  
Shepherd, D.S., Claussen, M.J., & Kurtz, S.E. 2001, *Science*, 292, 1513  
Stecklum, B., Käuffl, H.-U., Henning, Th., Feldt, M., Eckardt, A., & Nyman, L.Å. 1998, *ESO Press Release PR 08/98*  
Tamura, M., Gatley, I., Joyce, R.R., Ueno, M., & Sekiguchi, M. 1990, *ASP Conf. Ser. 14, Astrophysics with Infrared Arrays*, ed. R. Elston (San Francisco: ASP), 291  
Walsh, A.J., Burton, M., Hyland, A., & Robinson, G. 1998, *MNRAS*, 301, 640  
Walsh, A.J., Bertoldi, F., Burton, M.G., & Nikola, T. 2001 *MNRAS*, 326, 36  
Wardle, J.F.C. & Kronberg, P.P. 1974, *ApJ*, 194, 249  
Weintraub, D.A & Kastner, J. 1993, *ApJ*, 411, 767  
Yao, Y., Ishii, M., Nagata, T., Nakaya, H., & Sato, S. 2000, *ApJ*, 542, 392